CHAPTER 2

Dynamics Simulations of Photoinduced Proton Transfer Reactions of 2-(2′-Hydroxyphenyl)benzoxazole in the Gas Phase and Its Hydrated Clusters

2.1 Introduction

The excited-state intramolecular proton transfer (ESIntraPT) is one of the most fundamental and important processes due to its photophysical properties [31-33]. The applications of ESIntraPT are found in many applications such as organic light emitting diodes [3], luminescent materials [4, 5], and fluorescence sensings [6, 7]. Most of the ESIntraPT processes occur in molecules having a strong intramolecular hydrogen bond between the acidic proton (O–H, $–NH_2$) and the basic moiety (C=N, C=O), and the suitable geometry such as 2-(2′-hydroxyphenyl)benzoxazole (HBO) [37, 56, 66, 67, 72, 91-93], 2-(2′-hydroxyphenyl)benzothiazole (HBT) [58, 59, 64, 94-96], and 2-(2′-hydroxyphenyl)benzimidazole (HBI) [60, 61]. Generally in the ground state, the enol form of those molecules is stable because the phenolic proton is not acidic enough to be deprotonated, implying that tautomerization does not occur in the ground state [37]. Upon photoexcitation, however, the proton transfer (PT) reaction from the excited enol occurs to give the excited keto tautomer in sub-picosecond timescale [37, 56, 66, 67, 72, 91-93] (Figure 2.1). Among those molecules exhibiting ESIntraPT, HBO (in Figure 2.2) is found to be an interesting system [37, 56, 66, 67, 72, 91-93] because of its high quantum efficiency [64] compared to those of HBT and HBI. HBO comprises the hydroxyl group (O–H acting as a proton donor) and the benzoxazole group (a nitrogen atom acting as a proton acceptor). The O–H group of a proton donor and the N atom of an acceptor in HBO form an intramolecular hydrogen bond and exhibit a large Stokes shift arising from ESIntraPT [37, 56, 66, 67, 72, 91-93].

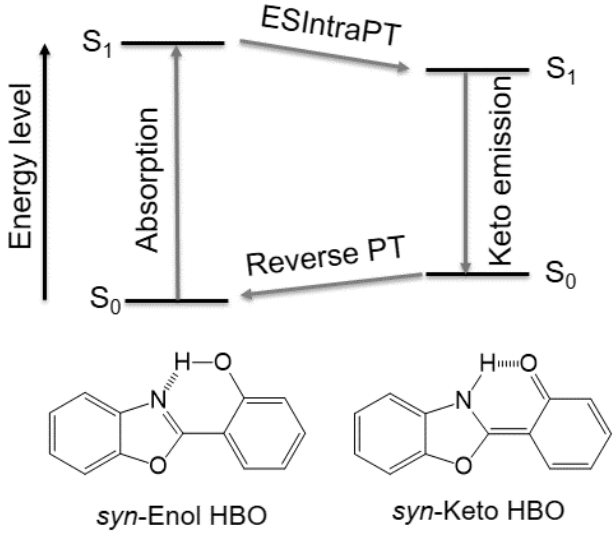

Figure 2.1 Scheme of excited-state intramolecular proton transfer (ESIntraPT) of HBO.

To utilize HBO as fluorescent sensors or fluorescent probing materials, the complete understanding of its photophysical properties of ESIntraPT in the gas phase and in solution is important [67, 93, 97, 98]. Possible conformations of enol HBO have been identified [56, 97] as shown in Figure 2.2a: *syn*-HBO or **I** (intramolecular O–H···N hydrogen bond), *anti*-HBO or **II** (intramolecular O–H···O hydrogen bond), and opened HBO or **III** (no intramolecular hydrogen bond) and only *syn*-HBO (**I**) can give the keto tautomer through the ESIntraPT process [4, 56, 66, 67, 97]. This process is known to occur on a femtosecond timescale [98] and the time constant of 60±30 fs (in cyclohexane) of *syn*-HBO (**I**) using time-resolved spectrometry was reported [91]. It has been observed that in the presence of polar solvents, especially polar protic solvents, the formation of strong intermolecular hydrogen bond between HBO and solvents might play a significant role in changing its photophysical characteristics [67, 93, 97, 98]. For solvated enol HBO, the formations of inter- and intramolecular hydrogen bonds between HBO and solvents are shown in Figure 2.2b: intramolecular hydrogen-bonded structure or **IV** (without an intermolecular hydrogen-bonded network), intermolecular hydrogen-bonded structure or **V** (water forming an intermolecular hydrogen-bonded network between the –OH and –N atom in the benzoxazole moiety), and opened-HBO or **VI** (intermolecular hydrogen bonding with water). Moreover, different PT pathways

either ESIntraPT or excited-state intermolecular PT (ESInterPT) can occur depending on the initial structure.

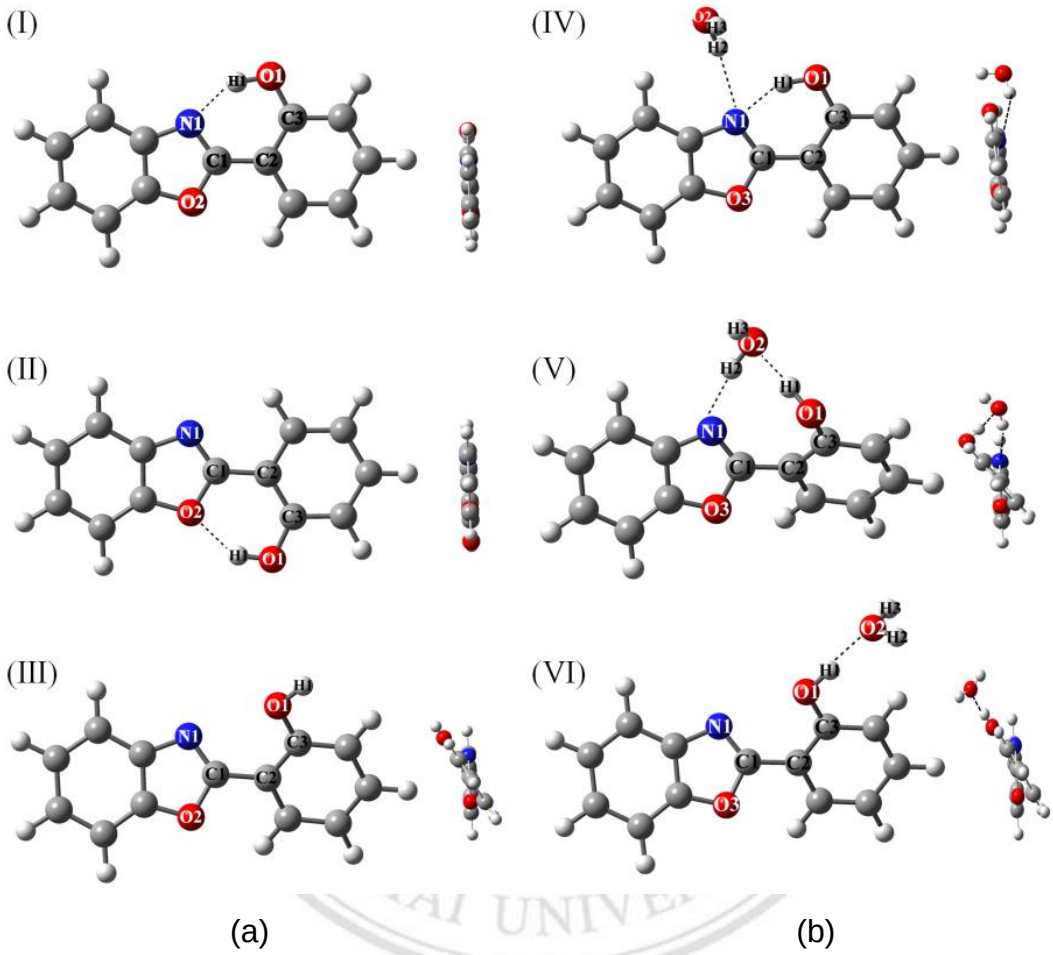

Figure 2.2 Ground-state optimized structures of HBO and its hydrated cluster computed at RI-ADC(2)/SVP-SV(P) level. (a) HBO [HBO (*syn*, **I**), HBO (*anti*, **II**), HBO (opened, **III**)] and (b) HBO(H_2O) [HBO(H_2O) (intramolecular hydrogen-bonded structure, **IV**), HBO(H_2O) (intermolecular hydrogen-bonded structure, **V**), HBO(H_2O) (opened, **VI**)], adjacent figures are their side view.

In the literature, the experiment studies provide detailed information of structural and photophysical properties of HBO both in gas and solution phases. In the gas phase and non-polar solvents, HBO shows its absorption peaks in the region of 280-330 nm and only keto emission peak is found at ~480 nm [37]. While in polar solvent, its

absorption is blue-shifted compared to non-polar solvent and the enol and keto emission peaks [66, 67, 72, 93] are observed at ~360 nm and ~475 nm, respectively. Absorption spectra of HBO in low-energy region (310-340 nm) are attributed to the $\pi\pi^*$ transitions of *syn*-enol and *anti*-enol HBO [56]. From these findings, solvent certainly plays an important role in absorption and emission spectra. Theoretical studies on equilibrium structures of HBO have confirmed the stability of enol isomer in the ground state and keto tautomer in excited state [56, 69, 99-111]. The studies of rotamerism of HBO in the ground state have shown that the *syn*-enol is more stable by about 5.77 $kcal \cdot mol^{-1}$ than the *anti*-enol [108]. Moreover, TD-DFT calculations of UV-vis spectra of HBO have demonstrated a good agreement of the simulated absorption and emission wavelength with experiment [102, 108]. Even though many studies [56, 69, 99-111] have reported on structural and photophysical properties of HBO and its hydrated cluster in the ultrafast PT, their excited-state dynamics information has not been investigated yet. Recently, classical dynamics of HBT, closely related to HBO reveal the mechanism and pathway of ESIntraPT, especially, PT time of HBT is 36 fs (in gas phase) reported by Barbatti *et al*. [62, 94] which is in excellent agreement with experiment by Lochbrunner *et al*. [95] at 33 fs. For HBT with a small cluster of water, the PT time was found to be much slower ~120-200 fs [59]. Such dynamics simulations can serve as a powerful tool to clarify detailed mechanisms such as reaction pathways, time constants of the PT process.

To provide more complete pictures of ultrafast PT of HBO, dynamics simulations are required to investigate whether PT occurs through inter- or intramolecular hydrogen bond, which is difficult to be obtained from the experiment. Here, we explore ground-state structures of free HBO and its hydrated cluster to find equilibrium conformations undergoing tautomerization. We present both static and dynamics calculations for free HBO and its solvated cluster. Reaction pathways, reaction probabilities and time constants are discussed in details.

2.2 Computational Details

In ground state, all possible structures of HBO and HBO(H_2O) were optimized at the second-order Møller-Plesset perturbation theory (MP2) with resolution-of-the-identity (RI) approximation for the electron repulsion integrals [79, 80]. The split valence polarized (SVP) was assigned to heavy atoms and the hydrogen atom of the phenol moiety and hydrogen atoms involved in the hydrogen-bonded network and the split valence (SV(P)) basis set was assigned to the remaining atoms. This efficient SVP-SV(P) basis set has been used and tested in our previous studies [59, 112]. All optimized structures were confirmed to be minima on the ground-state surface by normal-mode analysis with all positive frequencies. These calculations were carried out using TURBOMOLE 5.10 [113]. Then, selected optimized geometries were used as initial geometries in dynamics photoexcitation.

The excited-state dynamics simulations at Algebraic Diagrammatic Construction scheme up to second order or ADC(2) were performed using a microcanonical ensemble using Born-Oppenheimer energies and gradients in NEWTON-X program [114, 115] interfaced with TURBOMOLE. The ADC(2) method, originally derived using diagrammatic perturbation theory [116, 117], can be expressed by the symmetric Jacobian $\mathbf{A}^{ADC(2)} = \frac{1}{2}(\mathbf{A}^{CIS(D\infty)} + (\mathbf{A}^{CIS(D\infty)})^{*})$, where $\mathbf{A}^{CIS(D_{\infty})}$ is the Jacobian of the CIS(D_∞) coupled-cluster approximation [80]. The ADC(2) excited-state energies correspond to the eigenvalues of the Jacobian, while the ground state energy is given by the MP2 method. Overall, the quality of ADC(2) is very similar to that obtained at coupled-cluster to approximated second order (CC2) level [80, 118, 119]. Due to the description of the ultrafast PT (sub-picosecond timescale), tunneling and nonadiabatic effects were discarded in this work. A sampling procedure using a harmonic-oscillator Wigner distribution for each normal mode was used for initial conditions. Fifty trajectories as a representative set for each system were simulated using a time step of 1 fs with maximal duration of 300 fs. This time period is long enough to cover an ultrafast PT process. In addition, each trajectory was classified reactions into two types: ESPT (pathway A: ESIntraPT and pathway B: ESInterPT) and no PT (no reactions can be observed or reach a crossing between the S_1 and S_0 states

before any PT). All active ESPT trajectories were analyzed. The analysis shows that the first excited state is always characterized by a ππ* transition. This implies that the dynamics along the first excited state takes place purely in the ππ* state, characterizing a PT process and there are rare contributions from nπ* states. However, no πσ* state is found in this work [59]. In latter case, those trajectories were excluded from the analysis. For characteristic points along the reaction pathways, Normal (N), Intermediary Structure (IS) for each PT (IS*n*), and final tautomer (T) were assigned. PT time is figured out by the time at the intersection of O1–H1 breaking bond and N1···H1 forming bond. Furthermore, details of dynamics simulations such as energy difference between S_0 and S_1 states, probabilities and time evolutions in the excited state were described by a statistical analysis.

2.3 Results and Discussion

2.3.1 Ground-State Calculations

Ground-state structures of all conformations (Figure 2.2) were optimized in the gas phase to predict the most stable geometry in the ground state. For HBO molecule, there are different conformers namely HBO (*syn*, **I**), HBO (*anti*, **II**), HBO (opened, **III**) in Figure 2.2a. Intramolecular hydrogen bonds formed in **I** and **II** conformations are presented by dashed lines in Figure 2.2a. For HBO with a water molecule, there are three different conformations: i) intramolecular hydrogen-bonded structure (**IV**), ii) intermolecular hydrogen-bonded structure (**V)** and iii) opened-HBO (**VI)** in Figure 2.2b. Selective bond distances and torsion angle are summarized in Table 2.1.

The intramolecular hydrogen bond (N1···H1) for **I** is 1.774 Å. This bond is not formed in **III**, since the H1 rotates out and its position is located too far from N1. N1C1C2C3 torsion angle between two rings (hydroxyl and benzoxazole) of **I** and **II** is 0° and 180° confirming that these two structures are planar. However, torsion angle of **III** is 31.6° indicating that its structure is nonplanar. Different energies of these three isomers are in the range of 12 kcal·mol^{-1} (Table 2.1). The energies of **II** and **III** are higher than that of **I** by 6.02 and 12.26 kcal·mol^{-1}, respectively. HBO (**I**) is the most stable structure (lowest energy) which is in good agreement with computational results reported by Syetov [108] at B3LYP/6-31G(d,p) and Abou-Zied [56] at MP2/6-31G(d). Therefore, *syn*-HBO or **I** is chosen as an initiating structure for the excited-state dynamics simulation.

For hydrated enol HBO (Figure 2.2b), there are different geometries: intramolecular hydrogen bonding (**IV**), intermolecular hydrogen bonding (**V**), and opened HBO (**VI**) with water. **IV** is found to be the lowest energy, whereas energy of **V** is found to be slightly higher than that of **IV** about 1 kcal·mol^{-1}, which is considered to be insignificantly different. The energy of **VI** is much higher than that of **IV** about 8 kcal·mol^{-1}. When adding water molecule into HBO, the intramolecular hydrogen bond (N1···H1) for **IV** increases by 0.028 Å compared to **I**. For **V** and **VI,** a broken intramolecular hydrogen bond (N1···H1) in

HBO is caused by new hydrogen bonds between a water molecule and the hydroxyl group of HBO. The hydrogen-bonding interaction between water and HBO molecules causes the changes in torsion angle of N1C1C2C3 from planarity by 6°, 39°, and 36° for **IV**, **V** and **VI**, respectively. The reason for larger deviations from planarity of **V** and **VI** is the larger flexibility of the intermolecular hydrogen bonds as compared to the intramolecular hydrogen bond. **IV** and **V** are further selected as starting conformations for dynamics simulations upon excitation to study the different pathways of PT reactions because they are appropriate candidates for the PT process and their energies are also not significantly different.

Table 2.1 Selected bond distances (Å) and torsional angle (degree) and ground-state relative energies (kcal·mol^{-1}) of HBO and HBO(H_2O) computed at RI-ADC(2)/SVP-SV(P) level.

	HBO			**HBO(H_2O)**		
	I	**II**	**III**	**IV**	**V**	**VI**
O1–H1	0.986	0.969	0.966	0.981	0.988	0.976
Intramolecular hydrogen bond (N1···H1)	1.774			1.802		
Intermolecular hydrogen bond (O2···H1)					1.694	
Intermolecular hydrogen bond (N1···H2)				2.216	1.830	
O1···N1	2.659		2.846	2.686	3.070	2.878
O1···O2				3.580	2.682	2.798
O2···N1				3.072	2.762	
N1C1C2C3	0.0	180.0	31.6	5.9	38.8	35.3
ΔE^a	0.00	6.02	12.26	0.00	1.00	8.11

[a] Relative energies (kcal·mol^{-1}) to structure **I** for HBO and to structure **IV** for HBO(H_2O)

2.3.2 Excited-State Dynamics Simulations

On-the-fly dynamics simulations on the first excited state of fifty trajectories for each chosen initial structures (**I**, **IV** and **V**) were performed at RI-ADC(2)/SVP-SV(P) level. An analysis of the excited-state dynamics simulations providing types of reactions, probabilities, PT time, and reaction pathways is summarized in Table 2.2.

2.3.2.1 2-(2′-Hydroxyphenyl)benzoxazole (HBO, I)

All fifty trajectories of **I** show the ESIntraPT reaction. Labeling atoms are similar to that in Figure 2.2a. The average value of breaking (O1-H1) and forming (N1···H1) bonds is shown in Figure 2.3a. The intersection between those two bonds indicates PT time constant at 28 fs. The shaded area in Figure 2.3a is standard deviations of average bonds referring to the time range of proton being transferred from 10 to 55 fs. This PT time is in good agreement with the experiment of 30-90 fs in cyclohexane [91]. The average value of torsion angle of N1C1C2C3 fluctuates from 0 to 4 degrees until 230 fs. After that, a significant change is observed up to 8 degrees, indicating that slightly twisting structure of HBO occurs as shown in Figure 2.3b. More details of the PT process are illustrated by snapshots of excited-state dynamics simulation of HBO at different time (Figure 2.4), in which a normal (N) form starts at 0 fs. The H1 atom departs from phenol to the N atom of benzoxazole (IS) at 28 fs then after 30 fs the tautomer is formed. The relative energy difference between S_1 and S_0 gradually starts to decrease after the completion of PT process is reached after about 50 fs. This relative energy difference drops to below 2 eV (Figure 2.3c) due to the slightly non-planar conformations of HBO. As it was also reported by Syetov [108], this is an implication that the internal conversion to the ground state is initiated. Because of limitations of the RI-ADC(2) method to describe such twisted structures, the dynamics close to conical intersections and the possibility of internal conversion were not further investigated.

Table 2.2 Summary of the excited-state dynamics analysis of HBO systems.

Conformer	ESPT ($\pi\pi^*$) [a]		No PT ($\pi\pi^*/S_0$) [a]	Probability	Pathway A	Pathway B	
	Intra	Inter			PT1 (fs)	PT1 (fs)	PT2 (fs)
HBO (**I**)	50			1.00	28 (10-55)		
HBO(H_2O) (**IV**)	50			1.00	43 (30-90)		
HBO(H_2O) (**V**)	13	32	5	0.90	193 (124-247)	53 (26-95)	70 (37-110)

[a] Number of the ESPT reaction trajectories

PT time range (fs) from standard deviations given in parentheses.

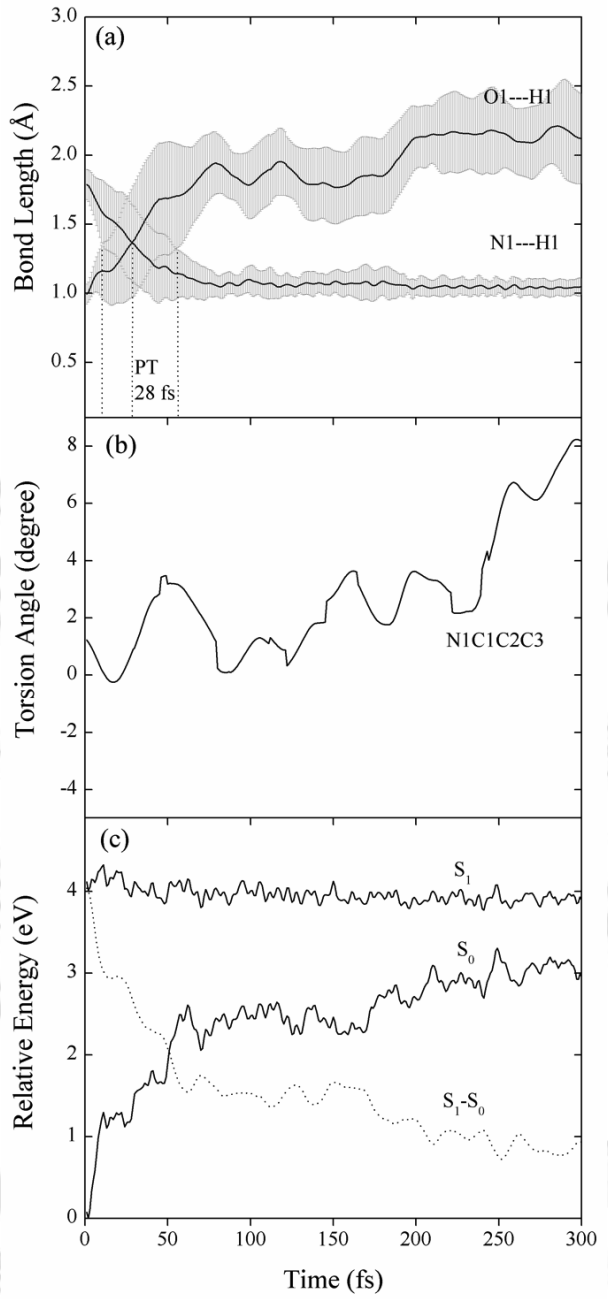

Figure 2.3 Average values of HBO (**I**). (a) Time evolution of average breaking and forming bonds. The shaded areas are the standard deviation. (b) Average torsion angle of N1C1C2C3 and (c) Average relative energies of excited state (S_1), ground state (S_0), and energy difference of S_1 and S_0 state (S_1-S_0).

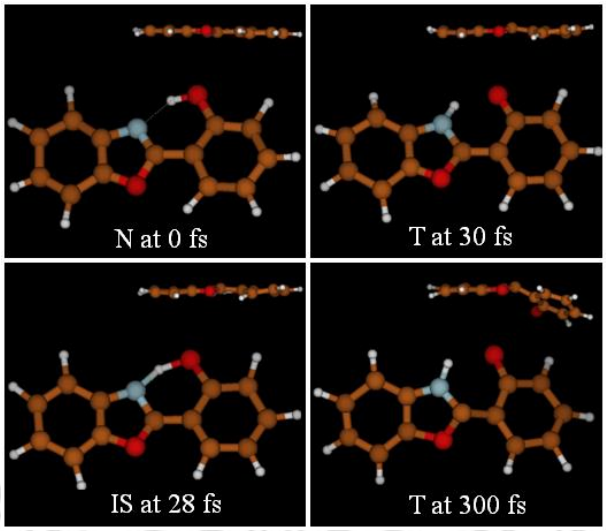

Figure 2.4 Snapshots of excited-state dynamics simulation of HBO or (**I**) at different time (up: top view, down: front view).

2.3.2.2 2-(2′-Hydroxyphenyl)benzoxazole with One Water Molecule (HBO(H_2O))

Two different conformations of HBO(H_2O): **IV** and **V**, were performed in the excited-state. An analysis of both cases is summarized in Table 2.2.

1. HBO(H_2O) Intramolecular Hydrogen-Bonded Structure (IV)

For the **IV** system, all trajectories show ESIntraPT with 100% of probability which is the same as **I** system. The similar analysis was done and results were given. The intersection of average breaking and forming bonds shows PT time at 43 fs within the time range of 30-90 fs (Table 2.2 and Figure 2.5a), which is about factor two slower than the free HBO. The explicit water in HBO(H_2O) plays a significant role in interacting with the hydroxyl of the phenol during the PT process, so that the PT time takes longer compared to that of no water in the **I** system. The average value of N1C1C2C3 slightly changes from 7° to 5° before 150 fs and keeps changing to 9° after 150 fs Figure 2.5b. From snapshots of excited-state dynamics simulation of **IV** (Figure 5), starting at 0 fs of N, at 43 fs IS is formed and after 46 fs the tautomer is achieved. The initial time of internal conversion begins after the tautomer is formed around 46 fs, which is faster than that of

I. The energy gap between S_1 and S_0 after completion of PT is lower than 2 eV, implying that the internal conversion initiates as shown in Figure 2.5c.

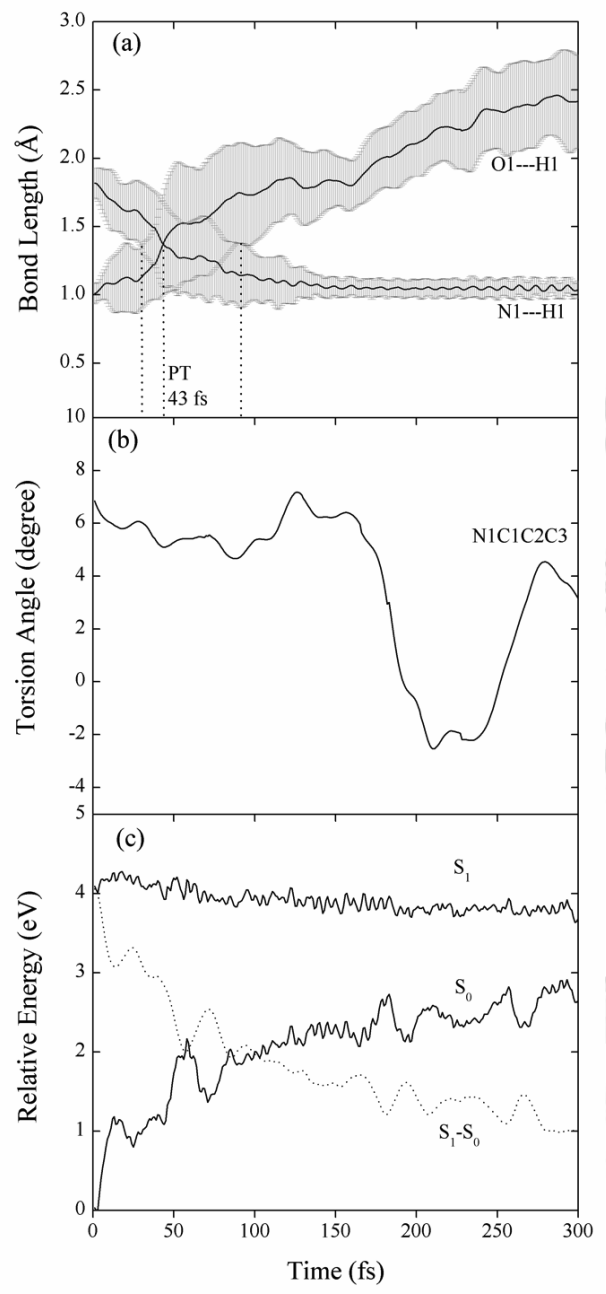

Figure 2.5 Average values of HBO (**IV**). (a) Time evolution of average breaking and forming bonds. The shaded areas are the standard deviation. (b) Average torsional angle of N1C1C2C3 and (c) Average relative energies of excited state (S_1), ground state (S_0), and energy difference of S_1 and S_0 state (S_1-S_0).

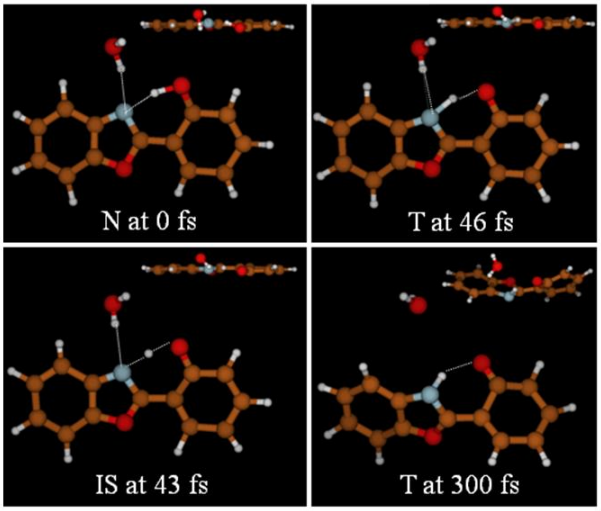

Figure 2.6 Snapshots of excited-state dynamics simulation of HBO(H_2O) or **IV** at different time (up: top view, down: front view).

2. HBO(H_2O) Intermolecular Hydrogen-Bonded Structure (V)

The analysis of fifty trajectories from excited-state dynamics simulations of **V** is summarized in TABLE 2.2. There are 32 out of 50 trajectories shows ESInterPT (64 %). However, intermolecular hydrogen-bonded structure rearranges itself to form intramolecular hydrogen-bonded structure during the dynamics (**V** changing to **IV**) for 13 trajectories (26 %). Five trajectories (10%) reach a crossing region between the S_1 and S_0 states before any PT could take place. These trajectories are excluded from the analysis. Because there are two possible pathways of PT, these two pathways are analyzed and discussed separately. The numbering atoms of **V** are the same as in Figure 2.2b.

For pathway A (ESIntraPT) of the starting structure **V** (intermolecular hydrogen bond), average value of the intersection lines between breaking and forming bonds for PT time is found at 193 fs (with the time range of 124-247 fs) is in TABLE 2.2 and shown in Figure 2.7a. The average value of N1C1C2C3 torsion decreases during the PT process as Figure 2.7b from about 40° (initial structure) to 0° (complete tautomerization). This torsion angle keeps decreasing down to -30°, indicating that a twisting of the

skeleton structure of HBO is taking place. And average value of energy gap (S_1 and S_0) gradually drops to 2 eV before 190 fs and then becomes lower than 2 eV (Figure 2.7c), corresponding to torsion twisting of HBO. This ESIntraPT process takes much longer time to complete, which is about factor four slower than that of **IV**. This slower PT is due to the competition between the formations of intramolecular hydrogen bond (forming **IV**) and intermolecular hydrogen bond (remaining original **V**) of water and HBO, in which the hydrogen bond rearrangement of H_2O takes place around 193 fs to form the intramolecular hydrogen bond and PT is reached at 195 fs as shown in Figure 2.8a.

For pathway B (ESInterPT) of the starting structure **V** (intermolecular hydrogen bond), the proton transfers from its original structure through hydrogen-bonded network. The PT process is described in two steps: (1) H1 moves from O1 to O2 at 53 fs (with the time range of 26-95 fs) and (2) H2 moves from O2 to N1 at 70 fs (with the time range of 37-110 fs) as given in TABLE 2.2 and shown in Figure 2.7d. The average value of N1C1C2C3 torsion slightly decreased from 40° (already twisted structure) to about 30° during the PT of 50-80 fs then keeps decreasing to about 10° (Figure 2.7e). Despite starting from the same initial structure, the change of N1C1C2C3 torsion of pathway B during the PT process is smaller than that of pathway A. This is because ESInterPT can occur through the already twisted structure without changing its skeleton structure back to planar like in the case of the **IV** and **V** (pathway A). The energy gap between S_1 and S_0 is lower than 2 eV after the tautomerization similar to the case of pathway A (Figure 2.7f). Snapshots of the excited-state dynamics simulation of HBO(H_2O) for pathway B are shown in Figure 2.8b.

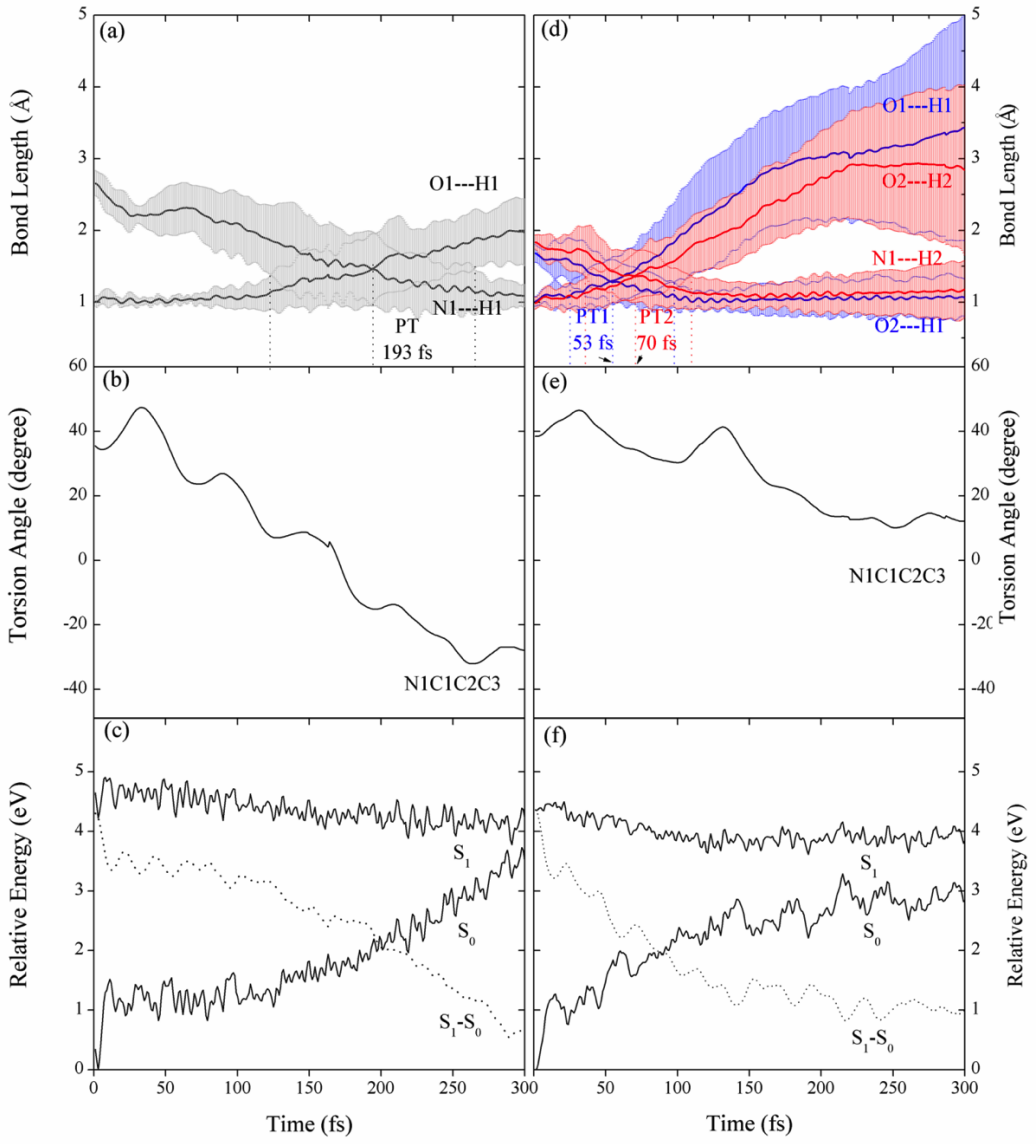

Figure 2.7 Average values of HBO(H_2O) (**V**). (a) Time evolution of average breaking and forming bonds for pathway A and (d) for pathway B. The shaded areas are the standard deviation. (b) Average torsional angle of N1C1C2C3 for pathway A and (e) for pathway B. (c) Average relative energies of excited state (S_1), ground state (S_0), and energy difference of S_1 and S_0 state (S_1-S_0) for pathway A and (f) for pathway B.

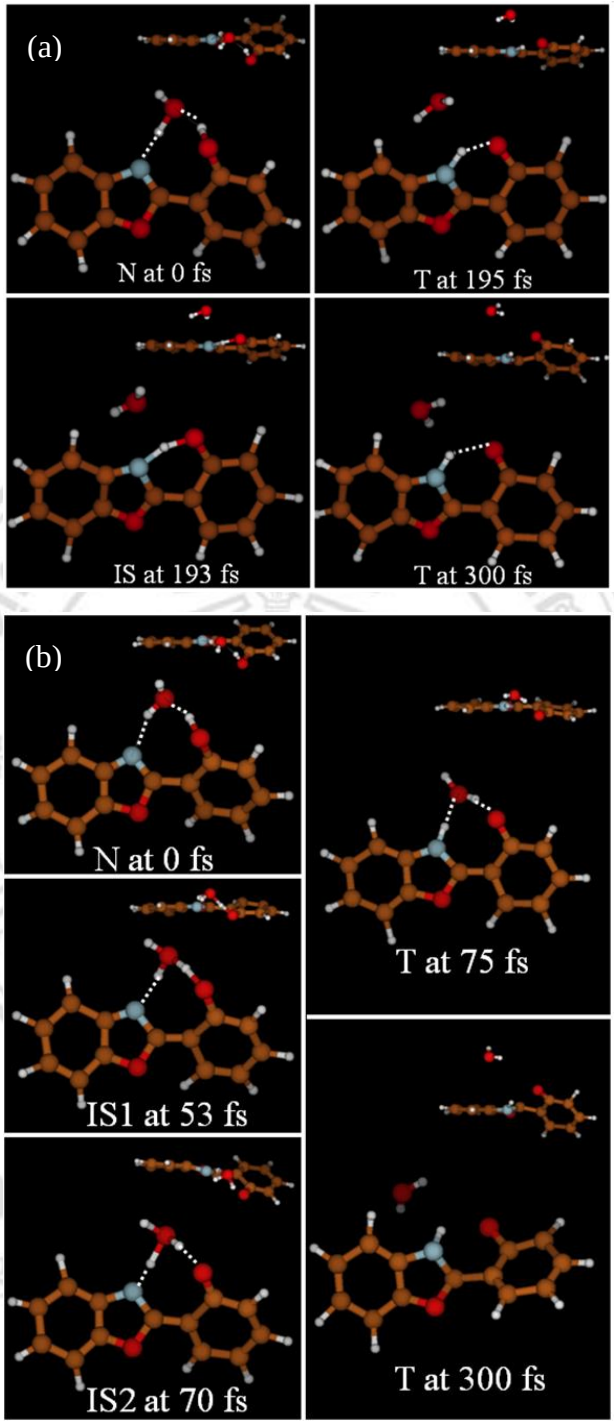

Figure 2.8 (a) Snapshots for pathway A and (b) for pathway B of the excited-state dynamics simulation of HBO(H_2O), **V** at different time
(up: top view, down: front view).

The PT time of the intramolecular hydrogen-bonding structure of HBO (**I**) taking place at about 28 fs is slightly faster than that of HBT at about 36 fs. These two PT times are insignificantly different (in the same range if the stand derivation is taken into account). The PT time of intermolecular hydrogen bonding structure of HBO (**V**) occurring within 70 fs is twice faster than that of HBT at 115 fs. In addition, the hydrogen bond rearrangement of intermolecular hydrogen bonding structure of HBO (**V**) takes place to form intramolecular hydrogen bonding (**V→IV**) and complete PT within 193 fs, which is insignificantly different from that of HBT at 205 fs. This implies that the hydrogen bond rearrangement of both HBO and HBT with water molecules requires the same amount of time prior to PT process. However, PT time of intramolecular hydrogen bonding structure (**IV**) of HBO is a factor two slower than that of HBT. This slower process of HBO can be explained by the weaker intramolecular hydrogen bond and only one water molecule is attached to HBO whereas three water molecules solvate the HBT. Three water molecules surrounding the HBT can stabilize the hydrogen bond much better than the one water [59, 94]. Overall, PT time of HBO systems is faster than that of the HBT. This is related to the electron-donating capacity of the heteroatoms, which is in the order of O > S [37]. Therefore, one water in HBO(H_2O) can be adequately used to clarify the role of water in competition of inter- and intramolecular hydrogen bonds.

2.4 Chapter Summary

The excited-state dynamics simulations were performed at RI-ADC(2)/SVP-SV(P) in the gas phase to study the enol-keto tautomerization in the excited state of free HBO and HBO(H_2O). Proton transfers of HBO systems along the first excited state take place in the $\pi\pi^*$ state. Free HBO undergoes ESIntraPT in ultrafast timescale of 28 fs which is in good agreement with the experiment. For hydrated HBO, there are two possible pathways depending on initial geometries of HBO(H_2O). In our dynamics simulations, structure **IV** of HBO(H_2O) as an intramolecular hydrogen-bonded structure shows ESIntraPT through its intrinsic intramolecular hydrogen bonding within 43 fs which is about factor two slower than the free HBO. Structure of HBO(H_2O) as an intermolecular hydrogen-bonded structure, however, shows two pathways: the first pathway is ESInterPT through its starting structure (intermolecular hydrogen-bonded network) within 70 fs and the second pathway is the hydrogen bond rearrangement of water of the starting structure to form the intramolecular hydrogen-bonded conformation of HBO before ESIntraPT occurs with longer time at 193 fs. This slower process in the latter pathway of HBO(H_2O) is the competition between the formations of intramolecular hydrogen bond (forming **IV**) and intermolecular hydrogen bond (remaining original **V**). Moreover, after tautomerization in the excited state is achieved, the twisted skeleton of structure **V** is found and confirmed by dramatically changes of torsion between two rings of phenol and benzoxazole moieties.